Waterlike thermodynamic anomalies in a repulsive-shoulder potential system

N. V. Gribova
Institute for High Pressure Physics, Russian Academy of Sciences, Troitsk 142190, Moscow Region, Russia and Institute for Computational Physics, Universität Stuttgart, Pfaffenwaldring 27, 70569 Stuttgart, Germany

Yu. D. Fomin
Institute for High Pressure Physics, Russian Academy of Sciences, Troitsk 142190, Moscow Region, Russia

Daan Frenkel
FOM Institute for Atomic and Molecular Physics, Amsterdam 1009 DB, The Netherlands and Department of Chemistry, University of Cambridge, Cambridge CB2 1EW, United Kingdom

V. N. Ryzhov
Institute for High Pressure Physics, Russian Academy of Sciences, Troitsk 142190, Moscow Region, Russia and Moscow Institute of Physics and Technology (State University), Dolgoprudny 141700, Moscow Region, Russia

(Received 23 January 2009; published 20 May 2009)

We report a computer-simulation study of the equilibrium phase diagram of a three-dimensional system of particles with a repulsive-shoulder potential. The phase diagram was obtained using free-energy calculations. At low temperatures, we observe a number of distinct crystal phases. We show that at certain values of the potential parameters the system exhibits the waterlike thermodynamic anomalies: a density anomaly and a diffusion anomaly. The anomalies disappear with increasing the repulsive step width: more precisely, their locations move to the region where the crystalline phase is stable.

DOI: 10.1103/PhysRevE.79.051202 PACS number(s): 61.20.Gy, 61.20.Ne, 64.60.Kw

Some liquids (for example, water, silica, silicon, carbon, and phosphorus) show anomalous behavior in the vicinity of their freezing lines [1–16]. The water phase diagrams have regions where a thermal expansion coefficient is negative (density anomaly), a self-diffusivity increases upon pressuring (diffusion anomaly), and the structural order of the system decreases upon compression (structural anomaly) [6,7]. The regions where these anomalies take place form nested domains in the density-temperature [6] (or pressure-temperature [7]) planes: the density anomaly region is inside the diffusion anomaly domain, and both of these anomalous regions are inside the broader structurally anomalous region. In the case of water these anomalies are usually related to the anisotropy of the intermolecular potential. However, isotropic potentials are also able to produce density and diffusion anomalies. It is interesting that such potentials may be purely repulsive and can be considered as the simplest models for the waterlike anomalies. It has been shown that waterlike structural, thermodynamic, and dynamic anomalies can be generated in systems where particles interact via isotropic potentials with two characteristic length scales, with shorter range corresponding to a hard-core-like steep repulsion and longer range representing softer repulsion—potentials in which two preferable interparticle distances compete depending on the thermodynamic conditions of the system [17–35]. In these studies it was found that pure repulsive-step potential showed no anomalies (see also [36]). However, recently it was shown that waterlike anomalies can exist in the systems of particles interacting through a purely repulsive step potential [37]. This finding is supported by a recent study by De Oliveira *et al.* [38] of the evolution of the waterlike anomalies in a system with a potential that is tunable from a "ramp" potential to a repulsive-step: the characteristic "water" anomalies were found in the ramp limit and all but one where found in the repulsive-step limit [36]. In this paper, De Oliveira *et al.* showed that potentials in which two preferred distances are present, always exhibit waterlike anomalies, be it that sometimes they may be in an inaccessible region, where the crystalline phase is more stable than the liquid. This is the case for the repulsive-step potential studied in Ref. [36].

The repulsive-shoulder potential was introduced in the early work of Hemmer and Stell [17,18] in order to describe isostructural phase transitions in materials such as Ce or Cs. It is the simplest example of a repulsive intermolecular potential that has a region of negative curvature in the repulsive part, a feature that is known to be present in the interatomic potentials of some pure metallic systems, metallic mixtures, electrolytes, and colloidal systems. Systems of particles interacting through such pair potentials can possess a rich variety of phase transitions and thermodynamic anomalies, including liquid-liquid phase transitions [39–41], and isostructural transitions in the solid region [42–44].

In the present paper, we show that waterlike anomalies do indeed exist for repulsive-shoulder potentials and we show how these anomalies move to the region where the liquid is metastable as the width of the repulsive step is increased. The width of the repulsive-shoulder potential studied in Refs. [36,38] corresponds to this limiting case.

The repulsive-shoulder potential has the form

$$\Phi(r) = \begin{cases} \infty, & r \le d \\ \varepsilon, & d < r \le \sigma \\ 0, & r > \sigma \end{cases} \tag{1}$$

where d is the diameter of the hard core, σ is the width of the repulsive step, and ε its height. In the low-temperature limit

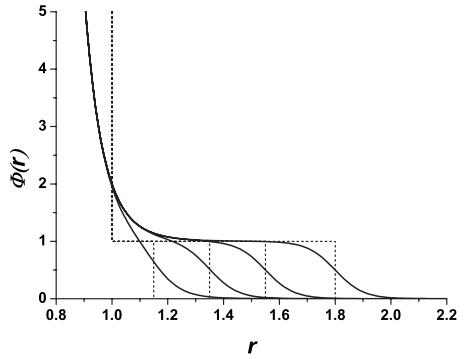

FIG. 1. A repulsive-shoulder potential consisting of a hard core plus a finite shoulder (dashed line) ($\varepsilon=1$, $\sigma=1.15,1.35,1.55,1.8$) along with the continuous version of potential (2) used in the simulations ($\varepsilon=1$, $\sigma_s=1.15,1.35,1.55,1.8$).

$\tilde{T}\equiv k_BT/\varepsilon \ll 1$ the system reduces to a hard-sphere system with hard-sphere diameter σ, while in the limit $\tilde{T}\gg 1$ the system reduces to a hard-sphere model with a hard-sphere diameter d. For this reason, melting at high and low temperatures follows simply from the hard-sphere melting curve $P=cT/\sigma'^3$, where $c\approx 12$ and σ' is the relevant hard-sphere diameter (σ and d, respectively). A changeover from the low-T to high-T melting behavior should occur for $\tilde{T}=\mathcal{O}(1)$. The precise form of the phase diagram depends on the ratio $s\equiv\sigma/d$. For large enough values of s one should expect to observe in the resulting melting curve a maximum that should disappear as $s\to 1$ [44]. The phase behavior in the crossover region may be very complex, as shown in [37].

In the present simulations we have used a smoothed version of the repulsive-shoulder potential [Eq. (1)], which has the form

$$\Phi(r)=\left(\frac{d}{r}\right)^n+\frac{1}{2}\varepsilon\{1-\tanh[k_0(r-\sigma_s)]\}, \tag{2}$$

where $n=14$, $k_0=10$. We have considered the following values of σ_s: $\sigma_s=1.15,1.35,1.55,1.8$. In Fig. 1 the repulsive-shoulder potential is shown along with its smooth version which was used in our Monte Carlo (MC) and molecular dynamics (MD) simulations.

In the remainder of this paper we use the dimensionless quantities: $\tilde{\mathbf{r}}\equiv\mathbf{r}/d$, $\tilde{P}\equiv Pd^3/\varepsilon$, and $\tilde{V}\equiv V/Nd^3\equiv 1/\tilde{\rho}$. As we will only use these reduced variables, we omit the tildes.

In Ref. [37], phase diagrams of repulsive-step models were reported for $\sigma_s=1.15,1.35,1.55$. In the present paper we also calculate the phase diagram of the system for $\sigma_s=1.8$. To determine the phase diagram at nonzero temperature, we performed *NVT* MD simulations combined with free-energy calculations. For equilibration rescaling of the velocities was used, for sampling we used *NVE* ensemble monitoring the stability of the temperature. In all cases, periodic boundary conditions were used. The number of particles varied between 250, 500, and 864. No system-size dependence of the results was observed. The system was equilibrated for 5×10^6 MD time steps. Data were subsequently collected during $3\times 10^6\delta t$ where the time step $\delta t=5\times 10^{-5}$.

In order to map out the phase diagram of the system, we computed its Helmholtz free energy using thermodynamic integration: the free energy of the liquid phase was computed via thermodynamic integration from the dilute gas limit [45], and the free energy of the solid phase was computed by thermodynamic integration to an Einstein crystal [45,46]. In the MC simulations of solid phases, data were collected during 5×10^4 cycles after equilibration. To improve the statistics (and to check for internal consistency) the free energy of the solid was computed at many dozens of different state points and fitted to multinomial function. The fitting function we used is $a_{p,q}T^pV^q$, where T and $V=1/\rho$ are the temperature and specific volume and powers p and q are connected through $p+q=N$. The value N we used for most of the calculations is 5. For the low-density fcc phase N was taken equal to 4, since we had less data points. The transition points were determined using a double-tangent construction.

The region where thermodynamic anomalies are expected is situated close to the region where the system undergoes structural arrest. As a consequence, proper sampling of the phase space can be problematic. To overcome this problem we used parallel tempering [45]. Instead of simulating a single system, we consider n systems, each running in the *NVT* ensemble at a different temperature. Systems at high temperatures go easily over potential barriers and systems at low temperatures sample the local free-energy minima. The idea of parallel tempering is to attempt Monte Carlo temperature swaps between the systems at different temperatures. If the low and high temperatures are far apart, the probability to accept such a swap move is quite low. For this reason, we use a range of "intermediate" temperatures. During a parallel tempering simulation, we generate equilibrium configurations for the system at all the temperatures in the simulation. In most cases, we used eight temperatures and tried to swap them 40 times. This simulation took almost 24 h running on eight processors in parallel at the Joint Supercomputing Center of Russian Academy of Sciences.

Figure 2 shows the phase diagrams that we obtain from the free-energy calculations for four different values of σ_s. In fact, the phase diagrams for $\sigma_s=1.15,1.35,1.55$ were already reported in Ref. [37]. We show these phase diagrams here too because they provide the "landscape" in which possible "water" anomalies should be positioned. Figure 2(a) shows the phase diagram of the system with $\sigma_s=1.15$. One can see that for the system with $\sigma_s=1.15$ there are no maxima in the melting curve. In a soft-sphere system described by the potential $1/r^{14}$ a face-centered-cubic crystal structure has been reported [47]. However, the addition of a small repulsive step leads to the appearance of the fcc-bcc transition shown in Fig. 2(a).

Figure 2(b) shows the phase diagram of the system with $\sigma_s=1.35$ in the ρ-T plane. There is a clear maximum in the melting curve at low densities. The phase diagram consists of two isostructural fcc domains corresponding to close packing of the small and large spheres separated by a sequence of structural phase transitions. This phase diagram was discussed in detail in our previous publication [37]. It is important to note that there is a region of the phase diagram where

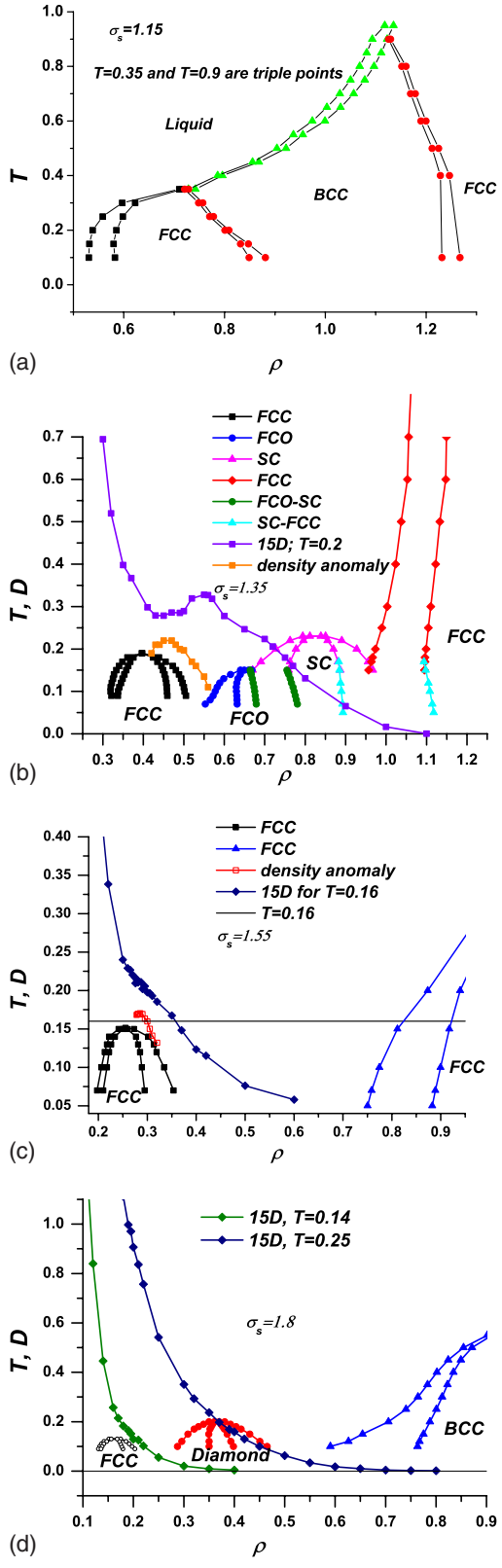

FIG. 2. (Color online) Phase diagram of the system of particles interacting through potential (2) with $\sigma_s=1.15, 1.35, 1.55, 1.8$ in ρ-T plane. Figures 2(b)–2(d) show the behavior of the diffusivity as a function density. In Figs. 2(b) and 2(c) one can see that it is nonmonotonic. We also indicate the density anomaly corresponding to the locations of the minima on the isochores (see Fig. 4).

we have not found any stable crystal phase. In that paper we argued that no simple crystal structure is stable in this density range because of frustration. The results of Ref. [37] suggest that a glass transition occurs in this region with $T_g=0.079$ at $\rho=0.53$. The apparent glass-transition temperature is above the melting point of the low-density fcc and FCO phases [see Fig. 2(b)]. If, indeed, no other crystalline phases are stable in this region, the "glassy" phase that we observe would be thermodynamically stable. This is rather unusual for one-component liquids. In simulations, glassy behavior is usually observed in metastable mixtures, where crystal nucleation is kinetically suppressed. One could argue that, in the glassy region, the present system behaves like a "quasi-binary" mixture of spheres with diameters d and σ_s and that the freezing-point depression is analogous to that expected in a binary system with a eutectic point: there are some values of the diameter ratio such that crystalline structures are strongly unfavorable and the glass phase could then be stable even at very low temperatures. The glassy behavior in the reentrant liquid disappears at higher temperatures.

One would expect frustration to be even more pronounced if we increase the step width. In Fig. 2(c) we show the phase diagram of the system with potential (2) for $\sigma_s=1.55$. This system also exhibits low- and high-density fcc phases separated by fcc to bcc transitions and the amorphous gap which is much more wider than for $\sigma_s=1.35$. We did not find any simple crystal structure between these isostructural phases. The glass transition temperature is $T_g=0.11091$ at $\rho=0.5$. One can see that the vitrification temperature becomes higher. Given the lack of crystal structure between crystalline phases and the increase in the glass transition temperature one can assume that the frustration effects become more pronounced with increase in the step width.

The phase diagram of the system with $\sigma_s=1.8$ is shown in Fig. 2(d). In this case a crystalline phase with diamond structure appears inside the disordered gap. However, this phase does not extend over the whole disordered region.

We expect that thermodynamic anomalies might occur in the vicinity of the "frustrated" part of the phase diagrams of the repulsive-step models. To check this, we calculated the isochores and the low-temperature diffusivity for different values of σ_s. The diffusivity was calculated in a conventional way [45] using the Einstein relation. It is proportional to the slope of the mean-squared displacement for long times, where mean-square displacement grows linearly with time. The model with $\sigma_s=1.15$ has no amorphous "gap" in the phase diagram and indeed we observe no anomalies in either D or ρ. In contrast, for other values of the potential parameters, we sometimes observe nonmonotonic behavior in D in the vicinity of the maximum of the melting curve [see Figs. 2(b) and 2(c)]. In Fig. 3 the behavior of the diffusivity is shown in more detail for different values of σ_s. One can see that with increasing the width of the repulsive step σ_s the anomaly is becoming less pronounced and disappears for $\sigma_s=1.8$. It is interesting to note that this value of σ_s corresponds to width of the repulsive step considered in [36,38] where no anomalies were found for the repulsive-shoulder potential.

The region where the diffusivity anomaly is observed almost coincides with a region where there is a minimum in

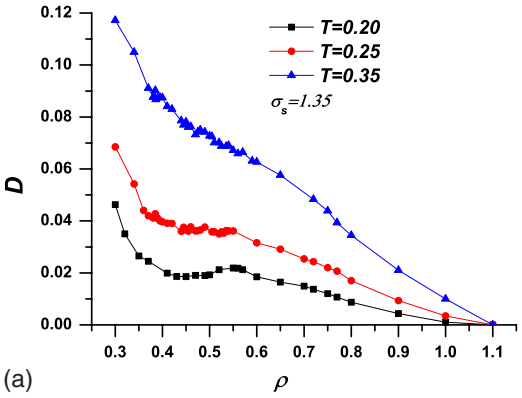

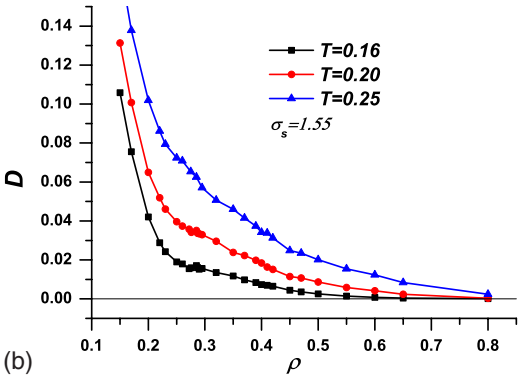

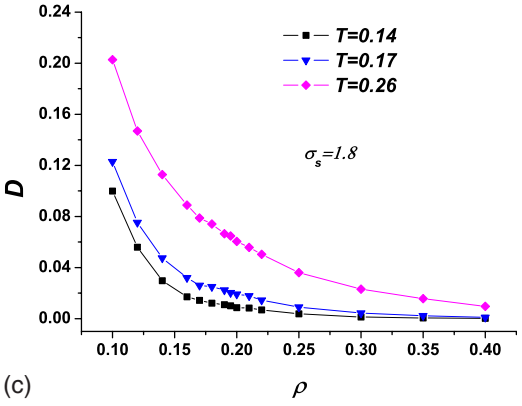

FIG. 3. (Color online) Diffusion anomaly for $\sigma=1.35, 1.55, 1.8$. One can see that the nonmonotonic behavior of diffusion at low temperatures (diffusion anomaly) decreases with increasing σ_s and disappears for $\sigma_s=1.8$.

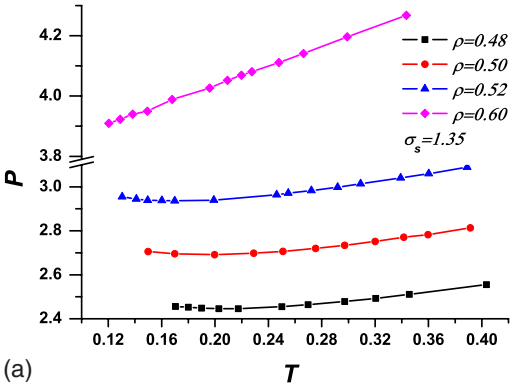

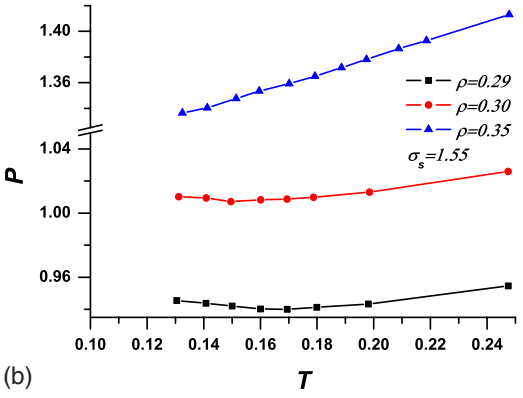

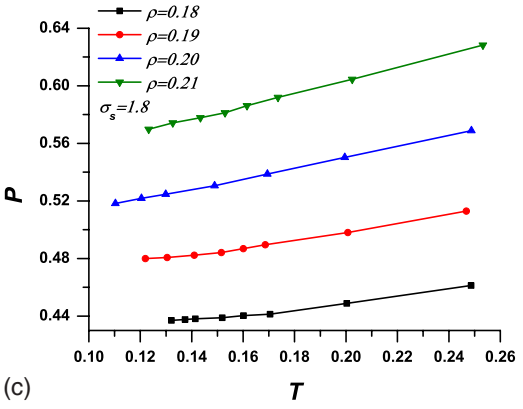

FIG. 4. (Color online) Density anomaly for $\sigma=1.35, 1.55, 1.8$. The low temperature minima on the isochores corresponding to negative thermal expansion coefficient become less developed with increasing σ_s and disappear for $\sigma_s=1.8$.

the curve of P versus T at constant ρ. Figures 2(b) and 2(c) show the locations of the pressure minima along the isochores. Figure 4 shows the corresponding $P-T$ curves. Using the thermodynamic relation $(\partial P/\partial T)_V=\alpha_P/K_T$, where α_P is a thermal expansion coefficient and K_T is the isothermal compressibility and taking into account that K_T is always positive and finite for systems in equilibrium not at a critical point, one can conclude that there is a range of densities and temperatures where the thermal expansion coefficient α_P is negative.

To elucidate the behavior of the anomalies with increasing the width of the repulsive step of the potential, we rescaled the parts of the phase diagrams corresponding to the first maximum on the melting curve (see Fig. 2) by multiplying the density by the σ_s^3 and dividing the temperature by $T_{\max}$, where $T_{\max}$ is the temperature corresponding to the maximum. In accordance with the qualitative picture depicted above the rescaled parts of the phase diagrams should coincide. As it can be seen in Fig. 5 this is roughly the case for $\sigma_s=1.35, 1.55, 1.8$. However, the curves do not collapse and, in fact, there is no reason why they should. In Fig. 5 we also show the locations of the minima of the isochores for $\sigma_s=1.35, 1.55$. One can see that with increasing width of the repulsive step the line of the minima moves to the melting line and then disappears into the metastable region. Unfortunately, we cannot analyze the behavior of the system in the metastable region because our simulation includes the paral-

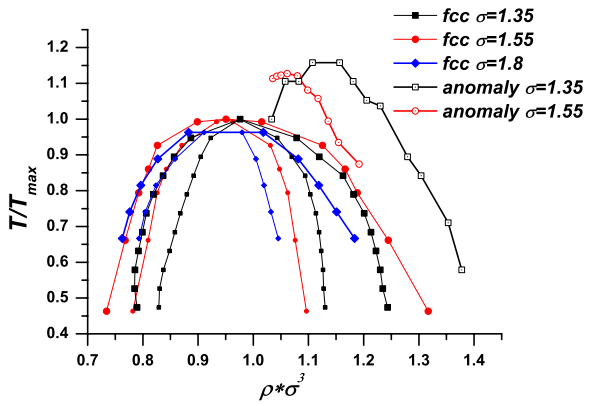

FIG. 5. (Color online) Rescaled part of the phase diagram corresponding to the maximum on the melting curve with locations of the minima on the isochores.

lel tempering approach which avoids the thermodynamically unstable states. It should be noticed that this scenario is in accordance with the observations of Ref. [38].

At low densities, we have effectively a liquid consisting of spheres with diameter σ_s, at high densities, the liquid consists of spheres with diameter d. In the "anomalous region" in between, our system appears as a mixture of both sorts of particles, and one can expect that in this region structural order should decrease for intermediate values of σ_s. In this case, the entropy of the system should increase with increasing density, and, due to the thermodynamic relation $(\frac{\partial \rho}{\partial T})_P = \rho^2 (\frac{\partial \rho}{\partial P})_T (\frac{\partial s}{\partial \rho})_T$ [48], one gets the anomalous behavior in this region. This further demonstrates that our model shows a quasibinary behavior.

In summary, we have performed extensive computer simulations of the phase behavior of three-dimensional systems described by a soft, purely repulsive-shoulder potential (2). We find a surprisingly complex phase behavior. We argue that the evolution of the phase diagram may be qualitatively understood by considering this one-component system as a quasibinary mixture of large and small spheres. Interestingly, the phase diagram includes two crystalline fcc domains separated by a sequence of the structural phase transitions and a reentrant liquid that becomes amorphous at low temperatures. Waterlike anomalies (density anomaly and diffusion anomaly) were found in the reentrant liquid for $\sigma_s = 1.35, 1.55$. The anomalies disappear with increasing the repulsive step width: their locations move to the region inside the crystalline phase in the vicinity of the maximum on the melting line.

We thank S. M. Stishov and V. V. Brazhkin for stimulating discussions. N.G. thanks A. Arnold for introduction to parallel computing and valuable remarks. N.G. and Y.F. thank the Joint Supercomputing Center of the Russian Academy of Sciences for computational power. The work was supported in part by the Russian Foundation for Basic Research (Grant No. 08-02-00781) and the Fund of the President of the Russian Federation for Support of Young Scientists (Grant No. MK-2905.2007.2). The work of the FOM Institute is part of the research program of FOM and is made possible by financial support from the Netherlands Organization for Scientific Research (NWO).

[1] P. Debenedetti, J. Phys.: Condens. Matter **15**, R1669 (2003).
[2] S. V. Buldyrev, G. Franzese, N. Giovambattista, G. Malescio, M. R. Sadr-Lahijany, A. Scala, A. Skibinsky, and H. E. Stanley, Physica A **304**, 23 (2002).
[3] C. A. Angell, Annu. Rev. Phys. Chem. **55**, 559 (2004).
[4] P. G. Debenedetti, *Metastable Liquids: Concepts and Principles* (Princeton University Press, Princeton, 1998).
[5] *New Kinds of Phase Transitions: Transformations in Disordered Substances*, Proc. NATO Advanced Research Workshop, Volga River, edited by V. V. Brazhkin, S. V. Buldyrev, V. N. Ryzhov, and H. E. Stanley (Kluwer, Dordrecht, 2002).
[6] J. R. Errington and P. G. Debenedetti, Nature (London) **409**, 318 (2001).
[7] P. A. Netz, F. V. Starr, H. E. Stanley, and M. C. Barbosa, J. Chem. Phys. **115**, 344 (2001).
[8] O. Mishima and H. E. Stanley, Nature (London) **396**, 329 (1998).
[9] C. A. Angell, E. D. Finch, and P. Bach, J. Chem. Phys. **65**, 3063 (1976).
[10] H. Thurn and J. Ruska, J. Non-Cryst. Solids **22**, 331 (1976).
[11] G. E. Sauer and L. B. Borst, Science **158**, 1567 (1967).
[12] F. X. Prielmeier, E. W. Lang, R. J. Speedy, and H.-D. Lüdemann, Phys. Rev. Lett. **59**, 1128 (1987).
[13] F. X. Prielmeier, E. W. Lang, R. J. Speedy, and H.-D. Lüdemann, Ber. Bunsenges. Phys. Chem. **92**, 1111 (1988).
[14] L. Haar, J. S. Gallagher, and G. S. Kell, *NBS/NRC Steam Tables: Thermodynamic and Transport Properties and Computer Programs for Vapor and Liquid States of Water in SI Units* (Hemisphere Publishing Co., Washington, DC, 1984), pp. 271–276.
[15] A. Scala, F. W. Starr, E. LaNave, F. Sciortino, and H. E. Stanley, Nature (London) **406**, 166 (2000).
[16] http://www.lsbu.ac.uk/water/anmlies.html
[17] P. C. Hemmer and G. Stell, Phys. Rev. Lett. **24**, 1284 (1970).
[18] G. Stell and P. C. Hemmer, J. Chem. Phys. **56**, 4274 (1972).
[19] G. Malescio, J. Phys.: Condens. Matter **19**, 073101 (2007).
[20] E. Velasco, L. Mederos, G. Navascues, P. C. Hemmer, and G. Stell, Phys. Rev. Lett. **85**, 122 (2000).
[21] P. C. Hemmer, E. Velasko, L. Mederos, G. Navascues, and G. Stell, J. Chem. Phys. **114**, 2268 (2001).
[22] M. R. Sadr-Lahijany, A. Scala, S. V. Buldyrev, and H. E. Stanley, Phys. Rev. Lett. **81**, 4895 (1998).
[23] M. R. Sadr-Lahijany, A. Scala, S. V. Buldyrev, and H. E. Stanley, Phys. Rev. E **60**, 6714 (1999).
[24] P. Kumar, S. V. Buldyrev, F. Sciortino, E. Zaccarelli, and H. E. Stanley, Phys. Rev. E **72**, 021501 (2005).
[25] L. Xu, S. V. Buldyrev, C. A. Angell, and H. E. Stanley, Phys. Rev. E **74**, 031108 (2006).
[26] E. A. Jagla, J. Chem. Phys. **111**, 8980 (1999); E. A. Jagla, Phys. Rev. E **63**, 061501 (2001).

[27] F. H. Stillinger and D. K. Stillinger, Physica A **244**, 358 (1997).
[28] A. Barros de Oliveira, P. A. Netz, T. Colla, and M. C. Barbosa, J. Chem. Phys. **124**, 084505 (2006).
[29] A. Barros de Oliveira, P. A. Netz, T. Colla, and M. C. Barbosa, J. Chem. Phys. **125**, 124503 (2006).
[30] A. Barros de Oliveira, M. C. Barbosa, and P. A. Netz, Physica A **386**, 744 (2007).
[31] J. Mittal, J. R. Errington, and T. M. Truskett, J. Chem. Phys. **125**, 076102 (2006).
[32] H. M. Gibson and N. B. Wilding, Phys. Rev. E **73**, 061507 (2006).
[33] P. J. Camp, Phys. Rev. E **71**, 031507 (2005).
[34] A. B. de Oliveira, G. Franzese, P. A. Netz, and M. C. Barbosa, J. Chem. Phys. **128**, 064901 (2008).
[35] L. Xu, S. V. Buldyrev, C. A. Angell, and H. E. Stanley, Phys. Rev. E **74**, 031108 (2006).
[36] A. Barros de Oliveira, P. A. Netz, and M. C. Barbosa, Eur. Phys. J. B **64**, 481 (2008).
[37] Yu. D. Fomin, N. V. Gribova, V. N. Ryzhov, S. M. Stishov, and Daan Frenkel, J. Chem. Phys. **129**, 064512 (2008).
[38] A. B. de Oliveira, P. A. Netz, and M. C. Barbosa, Europhys. Lett. **85**, 36001 (2009).
[39] V. N. Ryzhov and S. M. Stishov, Zh. Eksp. Teor. Fiz. **122**, 820 (2002) [JETP **95**, 710 (2002)].
[40] V. N. Ryzhov and S. M. Stishov, Phys. Rev. E **67**, 010201(R) (2003).
[41] Yu. D. Fomin, V. N. Ryzhov, and E. E. Tareyeva, Phys. Rev. E **74**, 041201 (2006).
[42] D. A. Young and B. J. Alder, Phys. Rev. Lett. **38**, 1213 (1977); D. A. Young and B. J. Alder, J. Chem. Phys. **70**, 473 (1979).
[43] P. Bolhuis and D. Frenkel, J. Phys.: Condens. Matter **9**, 381 (1997).
[44] S. M. Stishov, Philos. Mag. B **82**, 1287 (2002).
[45] Daan Frenkel and Berend Smit, *Understanding Molecular Simulation (From Algorithms to Applications)*, 2nd ed. (Academic Press, New York, 2002).
[46] D. Frenkel and A. J. Ladd, J. Chem. Phys. **81**, 3188 (1984).
[47] R. Agrawal and D. A. Kofke, Phys. Rev. Lett. **74**, 122 (1995).
[48] R. M. Lynden-Bell and P. G. Debenedetti, J. Phys. Chem. B **109**, 6527 (2005).